Int J Adv Manuf Technol (2001) 17:104–113

The International Journal of
Advanced
Manufacturing
Technology

Fixture Clamping Force Optimisation and its Impact on Workpiece Location Accuracy

B. Li and S. N. Melkote

George W. Woodruff School of Mechanical Engineering, Georgia Institute of Technology, Georgia, USA

Workpiece motion arising from localised elastic deformation at fixture–workpiece contacts owing to clamping and machining forces is known to affect significantly the workpiece location accuracy and, hence, the final part quality. This effect can be minimised through fixture design optimisation. The clamping force is a critical design variable that can be optimised to reduce the workpiece motion. This paper presents a new method for determining the optimum clamping forces for a multiple clamp fixture subjected to quasi-static machining forces. The method uses elastic contact mechanics models to represent the fixture–workpiece contact and involves the formulation and solution of a multi-objective constrained optimisation model. The impact of clamping force optimisation on workpiece location accuracy is analysed through examples involving a 3–2-1 type milling fixture.

Keywords: Elastic contact modelling; Fixture clamping force; Optimisation

1. Introduction

The location and immobilisation of the workpiece are two critical factors in machining. A machining fixture achieves these functions by locating the workpiece with respect to a suitable datum, and clamping the workpiece against it. The clamping force applied must be large enough to restrain the workpiece motion completely during machining. However, excessive clamping force can induce unacceptable level of workpiece elastic distortion, which will adversely affect its location and, in turn, the part quality. Hence, it is necessary to determine the optimum clamping forces that minimise the workpiece location error due to elastic deformation while satisfying the total restraint requirement.

Previous researchers in the fixture analysis and synthesis area have used the finite-element (FE) modelling approach or the rigid-body modelling approach. Extensive work based on the FE approach has been reported [1–8]. With the exception of DeMeter [8], a common limitation of this approach is the large model size and computation cost. Also, most of the FE-based research has focused on fixture layout optimisation, and clamping force optimisation has not been addressed adequately.

Several researchers have addressed fixture clamping force optimisation based on the rigid-body model [9–11]. The rigid body modelling approach treats the fixture-element and workpiece as perfectly rigid solids. DeMeter [12, 13] used screw theory to solve for the minimum clamping force. The overall problem was formulated as a linear program whose objective was to minimise the normal contact force at each locating point by adjusting the clamping force intensity. The effect of the contact friction force was neglected because of its relatively small magnitude compared with the normal contact force. Since this approach is based on the rigid body assumption, it can uniquely only handle 3D fixturing schemes that involve no more than 6 unknowns. Fuh and Nee [14] also presented an iterative search-based method that computes the minimum clamping force by assuming that the friction force directions are known *a priori*. The primary limitation of the rigid-body analysis is that it is statically indeterminate when more than six contact forces are unknown. As a result, workpiece displacements cannot be determined uniquely by this method.

This limitation may be overcome by accounting for the elasticity of the fixture–workpiece system [15]. For a relatively rigid workpiece, the location of the workpiece in the machining fixture is strongly influenced by the localised elastic deformation at the fixturing points. Hockenberger and DeMeter [16] used empirical contact force-deformation relations (called meta-functions) to solve for the workpiece rigid-body displacements due to clamping and quasi-static machining forces. The same authors also investigated the effect of machining fixture design parameters on workpiece displacement [17]. Gui et al [18] reported an elastic contact model for improving workpiece location accuracy through optimisation of the clamping force. However, they did not address methods for calculating the fixture–workpiece contact stiffness. In addition, the application of their algorithm for a sequence of machining loads representing a finite tool path was not discussed. Li and Melkote [19] and Hurtado and Melkote [20] used contact mechanics to

Correspondence and offprint requests to: Dr S. N. Melkote, George W. Woodruff School of Mechanical Engineering, Georgia Institute of Technology, Atlanta, Georgia 30332-0405, USA. E-mail: shreyes.melkote@me.gatech.edu

solve for the contact forces and workpiece displacement produced by the elastic deformation at the fixturing points owing to clamping loads. They also developed methods for optimising the fixture layout [21] and clamping force using this method [22]. However, clamping force optimisation for a multiclamp system and its impact on workpiece accuracy were not covered in these papers.

This paper presents a new algorithm based on the contact elasticity method for determining the optimum clamping forces for a multiclamp fixture–workpiece system subjected to quasi-static loads. The method seeks to minimise the impact of workpiece motion due to clamping and machining loads on the part location accuracy by systematically optimising the clamping forces. A contact mechanics model is used to determine a set of contact forces and displacements, which are then used for the clamping force optimisation. The complete problem is formulated and solved as a multi-objective constrained optimisation problem. The impact of clamping force optimisation on workpiece location accuracy is analysed via two examples involving a 3–2-1 fixture layout for a milling operation.

2. Fixture–Workpiece Contact Modelling

2.1 Modelling Assumptions

The machining fixture consists of L locators and C clamps with spherical tips. The workpiece and fixture materials are linearly elastic in the contact region, and perfectly rigid elsewhere. The workpiece–fixture system is subjected to quasi-static loads due to clamping and machining. The clamping force is assumed to be constant during machining. This assumption is valid when hydraulic or pneumatic clamps are used.

In reality, the elasticity of the fixture–workpiece contact region is distributed. However, in this model development, lumped contact stiffness is assumed (see Fig. 1). Therefore, the contact force and localised deformation at the ith fixturing point can be related as follows:

$$F_j^i = k_j^i \, d_j^i \tag{1}$$

where k_j^i $(j = x,y,z)$ denotes the contact stiffness in the tangential and normal directions of the local x_i,y_i,z_i coordinate frame, d_j^i $(j = x,y,z)$ are the corresponding localised elastic deformations along the x_i,y_i, and z_i axes, respectively, F_j^i $(j = x,j,z)$ represents the local contact force components with F_x^i and F_y^i being the local x_i and y_i components of the tangential force, and F_z^i the normal force.

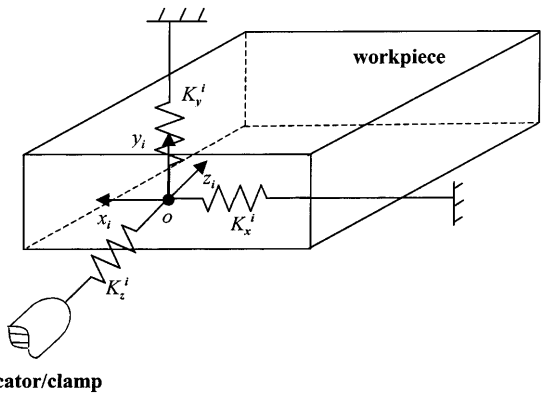

Fig. 1. A lumped-spring fixture–workpiece contact model. x_i, y_i, z_i, denote the local coordinate frame at the ith contact.

2.2 Workpiece–Fixture Contact Stiffness Model

The lumped compliance at a spherical tip locator/clamp and workpiece contact is not linear because the contact radius varies nonlinearly with the normal force [23]. The contact deformation due to the normal force P^i acting between a spherical tipped fixture element of radius R_i and a planar workpiece surface can be obtained from the closed-form Hertzian solution to the problem of a sphere indenting an elastic half-space. For this problem, the normal deformation Δ_n^i is given as [23, p. 93]:

$$\Delta_n^i = \left(\frac{9(P^i)^2}{16R_i(E^*)^2} \right)^{1/3} \tag{2}$$

where

$$\frac{1}{E^*} = \frac{1 - \nu_w^2}{\mathrm{E}_w} + \frac{1 - \nu_f^2}{E_f}$$

E_w and E_f are Young's moduli for the workpiece and fixture materials, respectively, and ν_w and ν_f are Poisson ratios for the workpiece and fixture materials, respectively.

The tangential deformation Δ_t^i $(= \Delta_{tx}^i$ or Δ_{ty}^i in the local x_i and y_i tangential directions, respectively) due to a tangential force Q^i $(= Q_x^i$ or $Q_y^i)$ has the following form [23, p. 217]:

$$\Delta_t^{ti} = \frac{Q^i}{8a_i} \left(\frac{2 - \nu_f}{G_f} + \frac{2 - \nu_w}{G_w} \right) \tag{3}$$

where

$$a_i = \left(\frac{3P^i \, R_i}{4} \left(\frac{1 - \nu_f}{E_f} + \frac{1 - \nu_w}{E_w} \right) \right)^{1/3}$$

and G_w and G_f are shear moduli for the workpiece and fixture materials, respectively.

A reasonable linear approximation of the contact stiffness can be obtained from a least-squares fit to Eq. (2). This yields the following linearised contact stiffness values:

$$k_z^i = 8.82 \left(\frac{16R_i \, (E^*)^2}{9} \right)^{1/3} \tag{4}$$

$$k_x^i = k_y^i = \frac{4}{E^*} \left(\frac{2 - \nu_j}{G_f} + \frac{2 - \nu_w}{G_w} \right)^{-1} k_z^i \tag{5}$$

In deriving the above linear approximation, the normal force P^i was assumed to vary from 0 to 1000 N, and the corresponding R^2 value of the least-squares fit was found to be 0.94.

3. Clamping Force Optimisation

The goal is to determine the set of optimal clamping forces that will minimise the workpiece rigid-body motion due to

localised elastic deformation induced by the clamping and machining loads, while maintaining the fixture–workpiece system in quasi-static equilibrium during machining. Minimisation of the workpiece motion will, in turn, reduce the location error.

This goal is achieved by formulating the problem as a multi-objective constrained optimisation problem, as described next.

3.1 Objective Function Formulation

Since the workpiece rotation due to fixturing forces is often quite small [17] the workpiece location error is assumed to be determined largely by its rigid-body translation $\mathbf{\Delta d}^w = [\Delta X^w\ \Delta Y^w\ \Delta Z^w]^T$, where ΔX^w, ΔY^w, and ΔZ^w are the three orthogonal components of $\mathbf{\Delta d}^w$ along the X_g, Y_g, and Z_g axes (see Fig. 2). The workpiece location error due to the fixturing forces can then be calculated in terms of the L_2 norm of the rigid-body displacement as follows:

$$\|\mathbf{\Delta d}^w\| = \sqrt{((\Delta X^w)^2 + (\Delta Y^w)^2 + (\Delta Z^w)^2)} \tag{6}$$

where $\|\ \|$ denotes the L_2 norm of a vector.

In particular, the resultant clamping force acting on the workpiece will adversely affect the location error. When multiple clamping forces are applied to the workpiece, the resultant clamping force, $\mathbf{P}_C^R = [P_X^R\ P_y^R\ P_Z^R]^T$, has the form:

$$\mathbf{P}_C^R = \mathbf{R}_C\ \mathbf{P}_C \tag{7}$$

where $\mathbf{P}_C = [P^{L+1}. . .P^{L+C}]^T$ is the clamping force vector, $\mathbf{R}_C = [\mathbf{n}_{L+1}. . .\mathbf{n}_{L+C}]^T$ is the clamping force direction matrix, $\mathbf{n}_{L+i} = [\cos\alpha_{L+i}\ \cos\beta_{L+i}\ \cos\gamma_{L+i}]^T$ is the clamping force direction cosine vector, and α_{L+i}, β_{L+i}, and γ_{L+i} are angles made by the clamping force vector at the ith clamping point with respect to the X_g, Y_g, Z_g coordinate axes ($i = 1,2,. . .,C$).

In this paper, the workpiece location error due to contact region deformation is assumed to be influenced only by the normal force acting at the locator–workpiece contacts. The frictional force at the contacts is relatively small and is neglected when analysing the impact of the clamping force on the workpiece location error. Denoting the ratio of the normal contact stiffness, k_z^i, to the smallest normal stiffness among all locators, k_z^s, by ξ_i ($i = 1,. . .,L$), and assuming that the workpiece rests on N_X, N_Y, and N_Z number of locators oriented in the X_g, Y_g, and Z_g directions, the equivalent contact stiffness in the X_g, Y_g, and Z_g directions can be calculated as

$$k_z^s\left(\sum_{i=1}^{N_X}\xi_i\right),\ k_z^s\left(\sum_{i=1}^{N_Y}\xi_i\right),\ \text{and}\ k_z^s\left(\sum_{i=1}^{N_Z}\xi_i\right)$$

respectively (see Fig. 3). The workpiece rigid-body motion, $\mathbf{\Delta d}^w$, due to clamping action can now be written as:

$$\mathbf{\Delta d}^w = \left[\frac{P_X^R}{k_z^s\left(\sum_{i=1}^{N_X}\xi_i\right)}\ \frac{P_Y^R}{k_z^s\left(\sum_{i=1}^{N_Y}\xi_i\right)}\ \frac{P_Z^R}{k_z^s\left(\sum_{i=1}^{N_Z}\xi_i\right)}\right]^T \tag{8}$$

The workpiece motion, and hence the location error can be reduced by minimising the weighted L_2 norm of the resultant clamping force vector. Therefore, the first objective function can be written as:

$$Minimize\ \|P_C^R\|_w = \sqrt{\left(\left(\frac{P_X^R}{\sum_{i=1}^{N_X}\xi_i}\right)^2 + \left(\frac{P_Y^R}{\sum_{i=1}^{N_Y}\xi_i}\right)^2 + \left(\frac{P_Z^R}{\sum_{i=1}^{N_Z}\xi_i}\right)^2\right)} \tag{9}$$

Note that the weighting factors are proportional to the equivalent contact stiffnesses in the X_g, Y_g, and Z_g directions.

The components of $\mathbf{P}_C^R$ are uniquely determined by solving the contact elasticity problem using the principle of minimum total complementary energy [15, 23]. This ensures that the clamping forces and the corresponding locator reactions are "true" solutions to the contact problem and yield "true" rigid-body displacements, and that the workpiece is kept in static equilibrium by the clamping forces at all times. Therefore, the minimisation of the total complementary energy forms the second objective function for the clamping force optimisation and is given by:

$$Minimise\ (U^* - W^*) = \frac{1}{2}\left[\sum_{i=1}^{L+C}\frac{(F_x^i)^2}{k_x^i} + \sum_{i=1}^{L+C}\frac{(F_y^i)^2}{k_y^i} + \sum_{i=1}^{L+C}\frac{(F_z^i)^2}{k_z^i}\right] \tag{10}$$

$$= \tfrac{1}{2}\boldsymbol{\lambda}^T\ \mathbf{Q}\boldsymbol{\lambda}$$

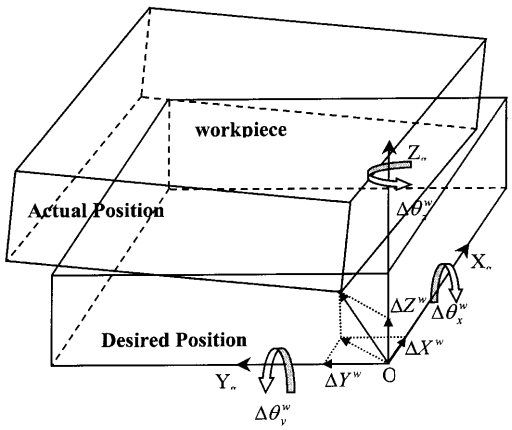

Fig. 2. Workpiece rigid body translation and rotation.

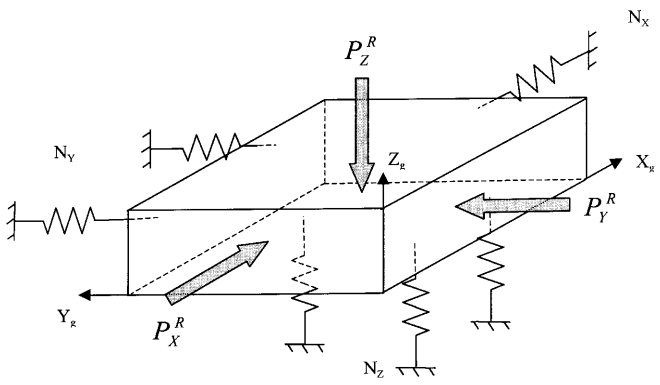

Fig. 3. The basis for the determination of the weighting factor for the L_2 norm calculation.

where U^* represents the complementary strain energy of the elastically deformed bodies, W^* represents the complementary work done by the external force and moments, $\mathbf{Q} = diag[c_x^1\ c_y^1\ c_z^1 \ldots c_x^{L+C}\ c_y^{L+C}\ c_z^{L+C}]$ is the diagonal contact compliance matrix, $c_j^i = (k_j^i)^{-1}$, and $\lambda = [F_x^1\ F_y^1\ F_z^1 \ldots F_x^{L+C}\ F_y^{L+C}\ F_z^{L+C}]^T$ is the vector of all contact forces.

3.2 Friction and Static Equilibrium Constraints

The optimisation objective in Eq. (10) is subject to certain constraints and bounds. Foremost among them is the static friction constraint at each contact. Coulomb's friction law states that $\sqrt{((F_x^i)^2 + (F_y^i)^2)} \leq \mu_s^i F_z^i$ (μ_s^i is the static friction coefficient). A conservative and linearised version of this nonlinear constraint can be used and is given by [19]:

$$|F_x^i| + |F_y^i| \leq \mu_s^i\ F_z^i \tag{11}$$

Since quasi-static loads are assumed, the static equilibrium of the workpiece is ensured by including the following force and moment equilibrium equations (in vector form):

$$\sum \mathbf{F} = \mathbf{0} \qquad \sum \mathbf{M} = \mathbf{0} \tag{12}$$

where the forces and moments consist of the machining forces, workpiece weight and the contact forces in the normal and tangential directions.

3.3 Bounds

Since the fixture–workpiece contact is strictly unilateral, the normal contact force, P^i, can only be compressive. This is expressed by the following bound on P^i:

$$P^i \geq 0 \quad (i = 1, \ldots, L + C) \tag{13}$$

where it is assumed that normal forces directed into the workpiece are positive.

In addition, the normal compressive stress at a contact cannot exceed the compressive yield strength (S_y) of the workpiece material. This upper bound is written as:

$$P^i \leq S_y\ A_i \quad (i = 1, \ldots, L+C) \tag{14}$$

where A_i is the contact area at the ith workpiece–fixture contact.

The complete clamping force optimisation model can now be written as:

$$Minimize\ \mathbf{f} = \begin{Bmatrix} f_1 \\ f_2 \end{Bmatrix} = \begin{Bmatrix} \frac{1}{2}\boldsymbol{\lambda}^T\mathbf{Q}\boldsymbol{\lambda} \\ \|\mathbf{P}_C^R\|_w \end{Bmatrix} \tag{15}$$

subject to: (11)–(14).

4. Algorithm for Model Solution

The multi-objective optimisation problem in Eq. (15) can be solved by the ϵ-constraint method [24]. This method identifies one of the objective functions as primary, and converts the other into a constraint. In this work, the minimisation of the complementary energy (f_1) is treated as the primary objective function, and the weighted L_2 norm of the resultant clamping force (f_2) is treated as a constraint. The choice of f_1 as the primary objective ensures that a unique set of feasible clamping forces is selected. As a result, the workpiece–fixture system is driven to a stable state (i.e. the minimum energy state) that also has the smallest weighted L_2 norm for the resultant clamping force.

The conversion of f_2 into a constraint involves specifying the weighted L_2 norm to be less than or equal to ϵ, where ϵ is an upper bound on f_2. To determine a suitable ϵ, it is initially assumed that all clamping forces are unknown. The contact forces at the locating and clamping points are computed by considering only the first objective function (i.e. f_1). While this set of contact forces does not necessarily yield the lowest clamping forces, it is a "true" feasible solution to the contact elasticity problem that can completely restrain the workpiece in the fixture. The weighted L_2 norm of these clamping forces is computed and taken as the initial value of ϵ. Therefore, the clamping force optimisation problem in Eq. (15) can be rewritten as:

$$Minimize\ f_1 = \tfrac{1}{2}\boldsymbol{\lambda}^T\mathbf{Q}\boldsymbol{\lambda} \tag{16}$$

subject to: $\|\mathbf{P}_C^R\|_w \geq \epsilon$, (11)–(14).

An algorithm similar to the bisection method for finding roots of an equation is used to determine the lowest upper bound for $\|\mathbf{P}_C^R\|_w$. By decreasing the upper bound ϵ as much as possible, the minimum weighted L_2 norm of the resultant clamping force is obtained. The number of iterations, K, needed to terminate the search depends on the required prediction accuracy δ and $|\epsilon|$, and is given by [25]:

$$K = \left\lceil \log_2 \left(\frac{|\epsilon|}{\delta} \right) \right\rceil \tag{17}$$

where $\lceil \bullet \rceil$ denotes the ceiling function. The complete algorithm is given in Fig. 4.

5. Determination of Optimum Clamping Forces During Machining

The algorithm presented in the previous section can be used to determine the optimum clamping force for a single load vector applied to the workpiece. However, during milling the magnitude and point of cutting force application changes continuously along the tool path. Therefore, an infinite set of optimum clamping forces corresponding to the infinite set of machining loads will be obtained with the algorithm of Fig. 4. This substantially increases the computational burden and calls for a criterion/procedure for selecting a single set of clamping forces that will be satisfactory and optimum for the entire tool path. A conservative approach to addressing these issues is discussed next.

Consider a finite number (say m) of sample points along the tool path yielding m corresponding sets of optimum clamping forces denoted as $\mathbf{P}_{opt}^1, \mathbf{P}_{opt}^2, \ldots, \mathbf{P}_{opt}^m$. At each sampling

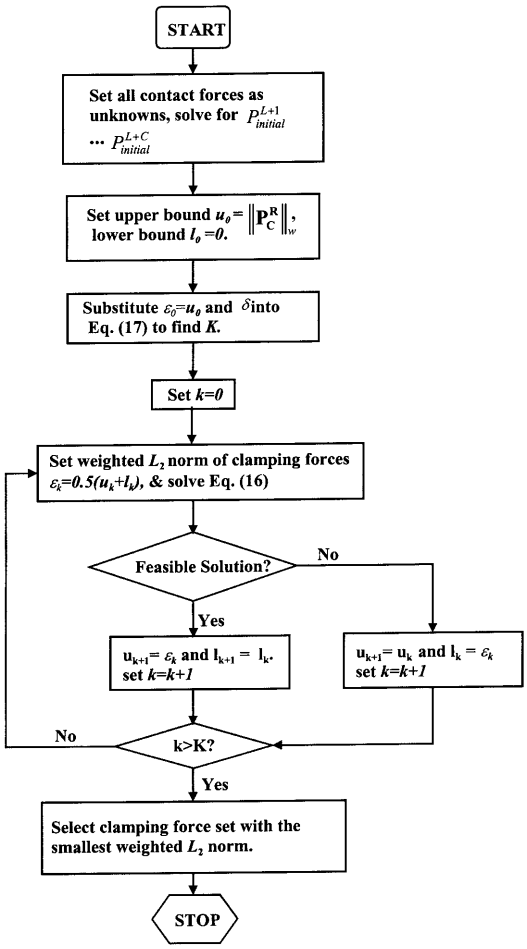

Fig. 4. Clamping force optimisation algorithm (used in example 1).

point, the following four worst-case machining load vectors are considered:

$$\begin{aligned}\mathbf{F}_{max}^{X} &= [F_X^{max}\ F_Y^1\ F_Z^1]^T \\ \mathbf{F}_{max}^{Y} &= [F_X^2\ F_Y^{max}\ F_Z^2]^T \\ \mathbf{F}_{max}^{Z} &= [F_X^3\ F_Y^3\ F_Z^{max}]^T \\ \mathbf{F}_{max}^{r} &= [F_X^4\ F_Y^4\ F_Z^4]^T\end{aligned} \tag{18}$$

where F_X^{max}, F_Y^{max}, and F_Z^{max} are the maximum X_g, Y_g, and Z_g components of the machining force, the superscripts 1, 2, 3 of F_X, F_Y, and F_Z stand for the other two orthogonal machining force components corresponding to F_X^{max}, F_Y^{max}, and F_Z^{max}, respectively, and $\|\mathbf{F}_{max}^r\| = \max(\sqrt{((F_X)^2 + (F_Y)^2 + (F_Z)^2)})$.

Although the four worst-case machining load vectors will not act on the workpiece at the same instant, they will occur once per cutter revolution. At conventional feedrates, the error introduced by applying the load vectors at the same point would be negligible. Therefore, in this work, the four load vectors are applied at the same location (but not simultaneously) on the workpiece corresponding to the sampling instant.

The clamping force optimisation algorithm of Fig. 4 is then used to calculate the optimum clamping forces corresponding to each sampling point. The optimum clamping forces have the form:

$$\mathbf{P}_{jmax}^i = [C_{1j}^i\ C_{2j}^i \ldots C_{Cj}^i]^T \quad (i = 1, \ldots, m) \quad (j = x,y,z,r) \tag{19}$$

where $\mathbf{P}_{jmax}^i$ is the vector of optimum clamping forces for the four worst-case machining load vectors, and C_{kj}^i ($k = 1,\ldots,C$) is the force magnitude at each clamp corresponding to the ith sample point and the jth load scenario.

After $\mathbf{P}_{jmax}^i$ is computed for each load application point, a single set of "optimum" clamping forces must be selected from all of the optimum clamping forces found for each clamp from all the sample points and loading conditions. This is done by sorting the optimum clamping force magnitudes at a clamping point for all load scenarios and sample points and selecting the maximum value, C_k^{max}, as given in Eq. (20):

$$C_k^{max} \le C_{kj}^i \quad (k = 1,\ldots,C) \tag{20}$$

Once this is complete, a set of optimised clamping forces $\mathbf{P}_{opt} = [C_1^{max}\ C_2^{max} \ldots C_C^{max}]^T$ is obtained. These forces must be verified for their ability to ensure static equilibrium of the workpiece–fixture system. Otherwise, more sampling points are selected and the aforementioned procedure repeated. In this fashion, the "optimum" clamping force, $\mathbf{P}_{opt}$, can be determined for the entire tool path. Figure 5 summarises the algorithm just described. Note that although this approach is conservative, it provides a systematic way of determining a set of clamping forces that minimise the workpiece location error.

6. Impact on Workpiece Location Accuracy

It is of interest to evaluate the impact of the clamping force algorithm presented earlier on the workpiece location accuracy. The workpiece is first placed on the fixture baseplate in contact with the locators. Clamping forces are then applied to push the workpiece against the locators. Consequently, localised deformations occur at each workpiece–fixture contact, causing the workpiece to translate and rotate in the fixture. Subsequently, the quasi-static machining load is applied causing additional motion of the workpiece in the fixture. The workpiece rigid-body motion is defined by its translation $\mathbf{\Delta d}^w = [\Delta X^w\ \Delta Y^w\ \Delta Z^w]^T$ and rotation $\mathbf{\Delta\theta}^w = [\Delta\theta_x^w\ \Delta\theta_y^w\ \Delta\theta_z^w)]^T$ about the X_g, Y_g, and Z_g axes (see Fig. 2).

As noted earlier, the workpiece rigid-body motion arises from the localised deformation, $\mathbf{d}^i = [d_x^i\ d_y^i\ d_z^i]^T$, at each fixturing point. Assuming that $\mathbf{r}_i = [X_i\ Y_i\ Z_i]^T$ describes the position vector of the ith locating point relative to the workpiece centre of mass, the coordinate transformation theorem can be used to express $\mathbf{d}^i$ in terms of the workpiece translation, $\mathbf{\Delta d}^w = [\Delta X^w\ \Delta Y^w\ \Delta Z^w]$, and workpiece rotation, $\mathbf{\Delta\theta}^w = [\Delta\theta_x^w\ \Delta\theta_y^w\ \Delta\theta_z^w]^T$, as follows:

$$\mathbf{d}^i = (\mathbf{R}_i^1)^T\ [\mathbf{R}(\mathbf{\Delta\theta}^w)\mathbf{r}_i + \mathbf{\Delta d}^w - \mathbf{r}_i] \tag{21}$$

where $\mathbf{R}_i^1$ denotes the rotation matrix describing the orientation of the local x_i, y_i, z_i coordinate frame at the ith contact relative to the global coordinate frame and $\mathbf{R}(\mathbf{\Delta\theta}_c^w)$ is a rotation matrix

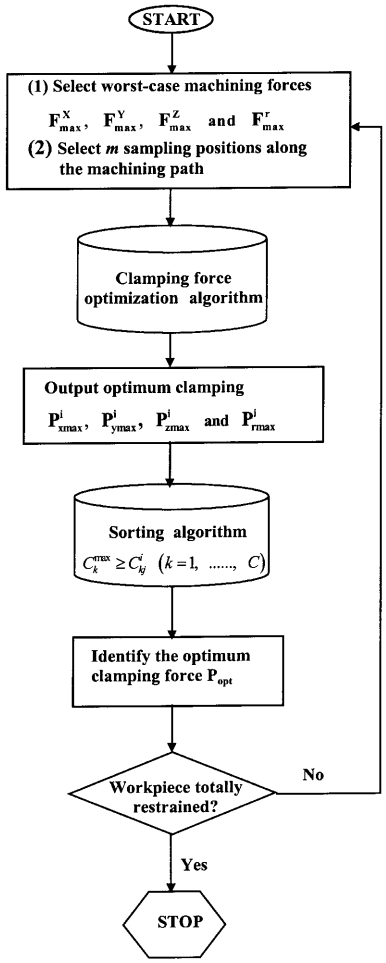

Fig. 5. The algorithm used in example 2.

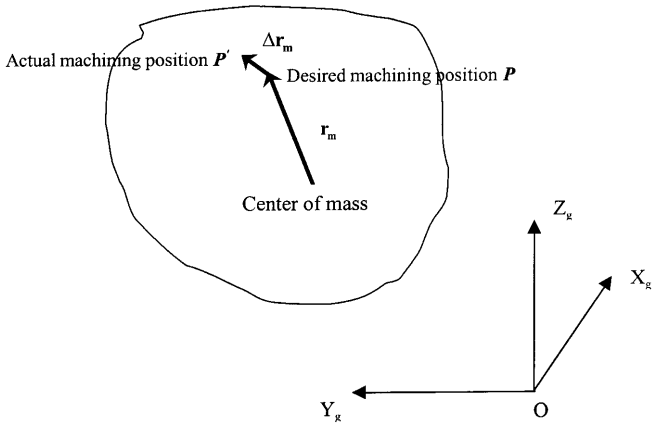

Fig. 6. The workpiece location error $\Delta\mathbf{r}_m$ due to clamping and machining.

defining the orientation of the workpiece fixed coordinate frame relative to the global coordinate frame.

Assuming that workpiece rotation within the fixture due to clamping, $\boldsymbol{\Delta}\theta^w$, is small, $\mathbf{R}(\boldsymbol{\Delta}\theta^w)$ can be approximated as:

$$\mathbf{R}(\boldsymbol{\Delta\theta}^w) = \begin{bmatrix} 1 & -\Delta\theta^w_z & \Delta\theta^w_y \\ \Delta\theta^w_z & 1 & -\Delta\theta^w_x \\ -\Delta\theta^w_y & \Delta\theta^w_x & 1 \end{bmatrix} \tag{22}$$

Equation (21) can now be rewritten as:

$$\mathbf{d}^i = (\mathbf{R}^1_i)^T\, \mathbf{B}^i\mathbf{q} \tag{23}$$

where

$$\mathbf{B}^i = \begin{bmatrix} 1 & 0 & 0 & 0 & Z_i & -Y_i \\ 0 & 1 & 0 & -Z_i & 0 & X_i \\ 0 & 0 & 1 & Y_i & -X_i & 0 \end{bmatrix}$$

is the transformation matrix obtained after re-arranging Eq. (21), and $\mathbf{q} = [\Delta X^w\ \Delta Y^w\ \Delta Z^w\ \Delta\theta^w_x\ \Delta\theta^w_y\ \Delta\theta^w_z]^T$ is the workpiece rigid-body motion vector due to clamping and machining.

The unilateral nature of the workpiece–fixture contact implies that no tensile forces are possible at a workpiece–fixture contact. Hence, the contact forces $\mathbf{F}^i = [F^i_x\ F^i_y\ F^i_z]^T$ at the *i*th fixturing point can be related to $\mathbf{d}^i$ as follows:

$$\mathbf{F}^i = \begin{cases} -\mathbf{K}^i\mathbf{d}^i, & \delta z^i > 0 \\ 0, & \textit{otherwise} \end{cases} \tag{24}$$

where $\delta z^i = (\mathbf{e}_z)^T\ \mathbf{d}^i$ is the net normal deformation at the *i*th contact due to clamping and machining loads, and $\delta z^i > 0$ implies that the net deformation is compressive while a negative sign represents tensile deformation; $\mathbf{K}^i = diag[k^i_x\ k^i_y\ k^i_z]$ is the *i*th contact stiffness matrix expressed in the local coordinate frame, and $\mathbf{e}_z = [0\ 0\ 1]^T$ is a unit vector.

Since hydraulic/pneumatic clamps are assumed in this study, clamping force intensities in the normal direction remain constant under external machining loads. Therefore, Eq. (24) must be modified for the clamping points as:

$$\mathbf{F}^i = [F^i_x\ F^i_y\ P^i]^T \tag{25}$$

where P^i is the clamping force at the *i*th clamping point.

Letting $\mathbf{f}_E$ denote a 6×1 vector of the external machining forces and weight, and combining Eqs (23)–(25) with the static equilibrium equation, the following set of equations are obtained:

$$\sum_{i=1}^{L+C} \begin{bmatrix} (\mathbf{R}^1_i)\mathbf{F}^i \\ \mathbf{r}_i \otimes [(\mathbf{R}^1_i)\mathbf{F}_i] \end{bmatrix} + \mathbf{f}_E = 0 \tag{26}$$

where $\otimes$ denotes the cross-product operation. The workpiece rigid-body motion due to clamping and machining, $\mathbf{q}$, can be obtained by solving Eq. (26).

The workpiece location error vector, $\boldsymbol{\Delta}\mathbf{r}_m = [\Delta r^X_m\ \Delta r^Y_m\ \Delta r^Z_m]^T$ (see Fig. 6), can now be computed as follows:

$$\boldsymbol{\Delta}\mathbf{r}_m = \mathbf{B}^m\mathbf{q} \tag{27}$$

where $\mathbf{r}_m = [X_m\ Y_m\ Z_m]^T$ is the position vector of the machining point with respect to the workpiece centre of mass, and

$$\mathbf{B}^m = \begin{bmatrix} 1 & 0 & 0 & 0 & Z_m & -Y_m \\ 0 & 1 & 0 & -Z_m & 0 & X_m \\ 0 & 0 & 1 & Y_m & -X_m & 0 \end{bmatrix}$$

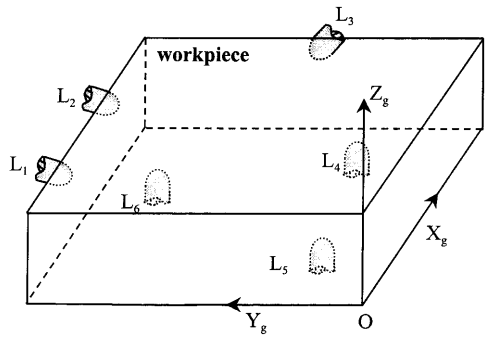

Fig. 7. The workpiece fixture configuration used in the simulation study. L_1–L_6, the workpiece fixture locator contacts; X_g, Y_g, Z_g, the global coordinate frame.

7. Simulation Work

The algorithm presented earlier was used to determine the optimum clamping forces and its impact on the workpiece accuracy for two example cases:

1. A single point force applied to the workpiece.
2. A sequence of quasi-static milling loads applied to the workpiece.

A 3–2-1 fixturing scheme shown in Fig. 7 was used to locate and hold a prismatic block of 7075-T6 aluminium (127 mm × 127 mm × 38.1 mm). The assumed layout for the spherical-tipped hard steel locators/clamps is given in Table 1. The static coefficient of friction for the workpiece–fixture material pair was taken to be 0.25.

The instantaneous end milling forces were computed using the EMSIM program developed at the University of Illinois [26] for the machining conditions given in Table 2. For example (1), the instantaneous machining forces were applied to the workpiece at the point (109.2 mm, 25.4 mm, 34.3 mm). The initial and optimum clamping forces were computed using the algorithm described in Fig. 4 and are given in Tables 3 and 4.

The algorithm shown in Fig. 5 was also tested. The milling of a 25.4 mm slot was simulated using EMSIM, with the cut starting at (0.0 mm, 25.4 mm, 34.3 mm) and ending at (127.0 mm, 25.4 mm, 34.3 mm) (see Fig. 8). The machining

Table 1. Fixture element position.

Fixture	Type of element tip	X (mm)	Y (mm)	Z (mm)
L1	Spherical	12.7	127.0	19.05
L2	Spherical	114.3	127.0	19.05
L3	Spherical	127.0	63.5	19.05
L4	Spherical	114.3	12.7	0.0
L5	Spherical	12.7	12.7	0.0
L6	Spherical	63.5	114.3	0.0
C1	Spherical	73.7	0.0	19.05
C2	Spherical	0.0	63.5	19.05
C3	Spherical	76.2	76.2	38.1

Note: L1–L6 are locators; C1–C2 are clamps. The tip radius is 5 mm.

Table 2. Machining conditions.

Condition	Feed (mm/tooth)	Axial depth (mm)	Radial depth (mm)	Spindle speed (r.p.m.)
1	0.2032	3.81	25.4	660
2	0.3048	3.81	25.4	660
3	0.4064	3.81	25.4	660

End mill: 25.4 mm diameter, 45° helix angle; 10° radial rake angle; 92.08 mm long; 4 flute coated carbide.

Table 3. Objective function value – example 1.

	Machining force			Algorithm parameters		Intial clamping force	Optimum clamping force
	F_x (N)	F_y (N)	F_z (N)	δ (N)	K	Weighted L_2 norm (N)	Weighted L_2 norm (N)
1	298.95	776.06	314.00	4.448	7	347.6	289.5
2	283.56	1105.67	442.10	4.448	7	503.0	392.1
3	443.69	1194.51	509.96	4.448	7	561.9	452.7

Note: Machining force is applied at (109.2 mm, 25.4 mm, 34.3 mm).

Table 4. Optimum clamping forces – example 1.

	Condition	Clamping force intensities (N)
Initial clamping force	1	(346.3, 211.2, 645.5)
	2	(470.9, 332.3, 885.7)
	3	(561.8, 345.3, 1028.6)
Optimum clamping force	1	(335.8, 66.1, 679.2)
	2	(433.9, 104.5, 928.4)
	3	(487.9, 99.3, 1104.7)

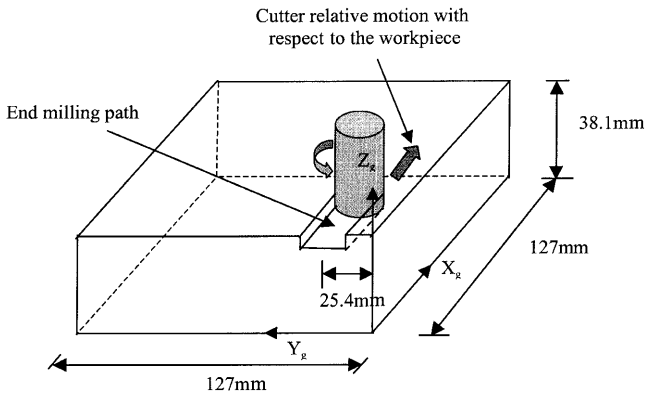

Fig. 8. The end milling process simulated for example 2.

Table 5. Worst-case machining loads for example 2.

	F_x (N)	F_y (N)	F_z (N)
$F^X_{\max}$	393.40	963.66	406.66
$F^Y_{\max}$	236.13	1116.58	421.46
$F^Z_{\max}$	331.52	1077.31	449.05
$F^r_{\max}$	283.56	1105.67	442.10

conditions used were the same as condition 2 in Table 2. The four worst-case machining load vectors were computed from the simulated milling force data and are given in Table 5. Five sampling points whose coordinates are listed in Table 6 were selected for the simulation. The optimum clamping force vector, $\mathbf{P}^i_{jmax}$ (= $\mathbf{P}^i_{xmax}$, $\mathbf{P}^i_{ymax}$, $\mathbf{P}^i_{zmax}$, $\mathbf{P}^i_{rmax}$), was calculated for each sampling point and load vector application, and the final optimum clamping force, $\mathbf{P}_{opt}$, was determined using the sorting algorithm discussed earlier.

8. Results and Discussion

The convergence of the optimum clamping force algorithm for example 1 is plotted in Fig. 9. For the fixture set-up assumed in this example (see Fig. 7), the weighted L_2 norm of the resultant clamping forces has the form $\|\mathbf{P}^R_C\|_w = \sqrt{((P^R_X/2)^2 + (P^R_Y)^2 + (P^R_Z/3)^2)}$. The results reveal that the optimum clamping forces under the stated machining conditions have a much lower weighted L_2 norm compared to the initial clamping force intensities. The initial clamping forces are those obtained at the start of the algorithm by minimising the complementary energy of the workpiece–fixture system.

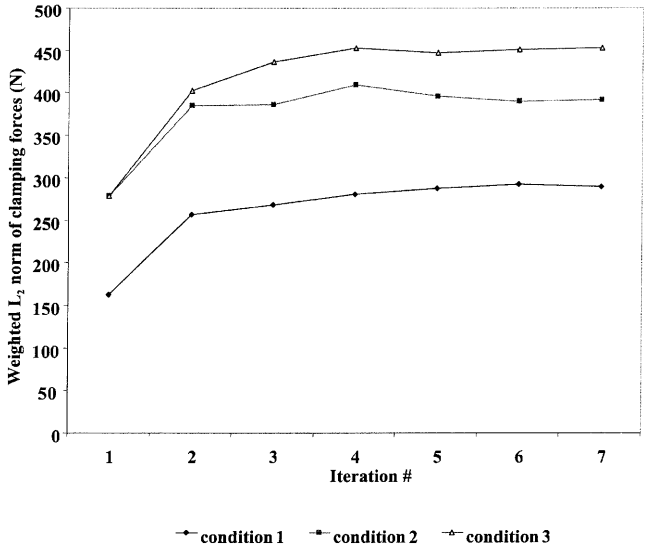

Fig. 9. Covergence characteristics of the algorithm for example 1.

The workpiece location errors due to clamping and the point load are given in Table 7. The results show that the workpiece rotation is small. The reduction in error at the machining point ranges from 13.1% to 14.6%. In this case, the improvement is not very large for all three machining conditions because the initial clamping force values determined from the minimisation of the complementary potential energy are close to the optimum clamping forces.

The algorithm of Fig. 5 was used in the second example where a sequence of milling loads was applied to the workpiece. The optimum clamping forces, $\mathbf{P}^i_{jmax}$ (=$\mathbf{P}^i_{xmax}$, $\mathbf{P}^i_{ymax}$, $\mathbf{P}^i_{zmax}$, $\mathbf{P}^i_{rmax}$), corresponding to each sample point are given in Table 6, along with the final optimum clamping force, $\mathbf{P}_{opt}$. The weighted L_2 norm of the initial and optimum clamping forces are plotted in Fig. 10, and at each sampling point, the weighted L_2 norm of $\mathbf{P}^i_{xmax}$, $\mathbf{P}^i_{ymax}$, $\mathbf{P}^i_{zmax}$, and $\mathbf{P}^i_{rmax}$ are plotted.

The results indicate that since every component of $\mathbf{P}_{opt}$ is the maximum among all the corresponding clamping force magnitudes, it has the maximum weighted L_2 norm. However, as shown in Fig. 10, if the maximum component at each clamping point is used for the initial clamping force, then the corresponding set of clamping forces, $\mathbf{P}_{ini}$, has a considerably larger weighted L_2 norm than $\mathbf{P}_{opt}$. Hence, $\mathbf{P}_{opt}$ is an improved solution for the complete tool path.

The above simulation results indicate that the approach presented in this paper can be used to optimise the clamping forces. In comparison to the initial clamping force intensity, this approach will reduce the weighted L_2 norm of the resultant clamping force, and will therefore improve the workpiece location accuracy.

Table 6. Optimum clamping forces – example 2.

Machining force application point (mm)	$\mathbf{p}^i_{jmax}$	Optimum clamping force (N)	Final weighted L_2 norm (N)
(21.2, 25.4, 34.3)	$\mathbf{p}^1_{xmax}$	(644.9, 312.2, 904.7	540.8
	$\mathbf{p}^1_{ymax}$	(680.6, 168.8, 1010.2)	507.6
	$\mathbf{p}^1_{zmax}$	(738.5 341.1, 954.5)	594.9
	$\mathbf{p}^1_{rmax}$	(716.3, 193.1, 1026.8)	531.7
(42.4, 25.4, 34.3)	$\mathbf{p}^2_{xmax}$	(479.2, 102.2, 972.7)	415.9
	$\mathbf{p}^2_{ymax}$	(583.5, 178.5, 936.5)	463.1
	$\mathbf{p}^2_{zmax}$	(529.3, 120.5, 1022.9)	448.1
	$\mathbf{p}^2_{rmax}$	(538.5, 145.3, 997.0)	451.7
(63.5, 25.4, 34.3)	$\mathbf{p}^3_{xmax}$	(386.3, 52.9, 918.7)	365.9
	$\mathbf{p}^3_{ymax}$	(412.2, 75.0, 911.1)	374.6
	$\mathbf{p}^3_{zmax}$	(450.0, 100.8, 945.4)	400.0
	$\mathbf{p}^3_{rmax}$	(433.9, 104.5, 928.4)	392.1
(84.7, 25.4, 34.3)	$\mathbf{p}^4_{xmax}$	(338.2, 126.0, 873.2)	359.4
	$\mathbf{p}^4_{ymax}$	(307.3, 192.1, 930.6)	395.9
	$\mathbf{p}^4_{zmax}$	(349.5, 171.4, 957.1)	402.1
	$\mathbf{p}^4_{rmax}$	(332.0, 186.1, 954.8)	404.3
(105.9, 25.4, 34.3)	$\mathbf{p}^5_{xmax}$	(230.1, 0.0, 863.9)	310.1
	$\mathbf{p}^5_{ymax}$	(265.5, 15.2, 958.1)	346.2
	$\mathbf{p}^5_{zmax}$	(276.0, 0.0, 973.7)	352.7
	$\mathbf{p}^5_{rmax}$	(277.3, 5.1, 979.6)	354.8
	$\mathbf{P}_{opt}$	(738.5, 341.1, 1026.8)	608.2

Table 7. Workpiece location error reduction – example 1.

		Resultant workpiece motion, q ($\times 10^{-3}$ mm, $\times 10^{-3}$ degree)	Error vector at the machining point $\Delta \mathbf{r}_m$ ($\times 10^{-3}$ mm)	Error vector magnitude, $\|\Delta \mathbf{r}_m\|$ ($\times 10^{-3}$ mm)	Error reduction (%)
Initial clamping force	1	(10.6 16.2 –4.5 –2.9 –2.8 3.5)	(12.0 17.1 –2.6)	21.1	
	2	(13.3 22.5 –5.7 –4.6 –4.7 3.6)	(14.2 24.0 –2.6)	28.1	
	3	(16.5 25.4 –6.8 –4.6 –4.6 5.2)	(18.5 26.9 –3.7)	32.8	
Optimum clamping force	1	(7.8 15.8 –9.1 1.3 –4.2 3.3)	(7.7 13.8 –9.0)	18.2	13.7
	2	(9.4 21.7 –12.0 1.2 –6.7 3.7)	(8.7 19.1 –11.5)	24.0	14.6
	3	(13.4 25.2 –9.6 –3.0 –3.2 5.4)	(14.4 23.6 –6.8)	28.5	13.1

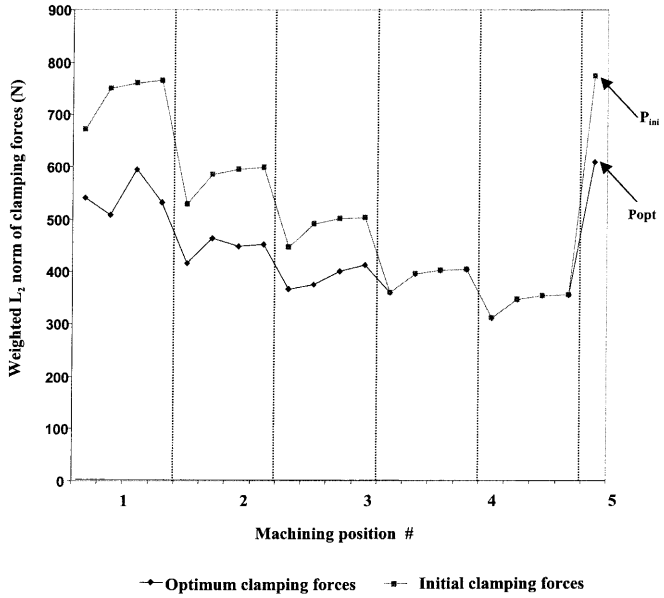

Fig. 10. Comparison of initial and optimum objective function values for example 2.

9. Conclusions

The paper presented a new method for determining the optimum clamping forces for a multiple clamp fixture–workpiece system subjected to quasi-static machining loads. The algorithm for clamping force optimisation is based on a contact mechanics model of the fixture–workpiece system and seeks to minimise the weighted L_2 norm of the resultant clamping force applied to the workpiece, and therefore the workpiece location error. The overall model is formulated as a bi-objective constrained optimisation problem and solved using the ϵ-constraint method. The algorithm was illustrated via two simulation examples involving a 3–2-1 type milling fixture with two clamps.

Future work will address optimisation of the fixture–workpiece system in the presence of dynamic loads where the inertia, stiffness, and damping effects play an important role in determining the workpiece–fixture system response characteristics.

References

1. J. D. Lee and L. S. Haynes, “Finite-element analysis of flexible fixturing system”, Transactions ASME, Journal of Engineering for Industry, 109, pp. 134–139.
2. W. Cai, S. J. Hu and J. X. Yuan, “Deformable sheet metal fixturing: principles, algorithms, and simulations”, Transactions ASME, Journal of Manufacturing Science and Engineering, 118, pp. 318–324, 1996.
3. P. Chandra, S. M. Athavale, R. E. DeVor and S. G. Kapoor, “Effect of preloads on the surface flatness during fixturing of flexible workpieces”, Proceedings of the Second S. M. Wu Symposium on Manufacturing Science, vol. 2, pp. 146–152, 1996.
4. R. J. Menassa and V. R. DeVries, “Optimization method applied to selecting support position in fixture design”, Transactions ASME, Journal of Engineering for Industry, 113, pp. 412–414, 1991.
5. A. J. C. Trappey, C. Su and J. Hou, “Computer-aided fixture analysis using finite-element analysis and mathematical optimization modeling”, ASME Proceedings, MED-31, pp. 777–787, 1995.
6. S. N. Melkote, S. M. Athavale, R. E. DeVor, S. G. Kapoor and J. Burkey, “Prediction of the reaction force system for machining fixtures based on machining process simulation”, Transactions of NAMRI/SME, 23, pp. 207–214, 1995.
7. Y. J. Liao, D. A. Stephenson and S. J. Hu, “Fixture layout optimization considering workpiece–fixture contact interaction; simulation results”, Transactions of NAMRI/SME, 26, pp. 341–346, 1998.
8. E. C. DeMeter, “Fast support layout optimization”, International Journal of Machine Tools and Manufacture, 38(10–11), pp. 1221–1239. 1998.
9. Y.-C. Chou, V. Chandru, M. M. Barash, “A mathematical approach to automatic configuration of machining fixtures: analysis and synthesis”, Transactions ASME, Journal of Engineering for Industry, 111(4), pp. 299–306, 1989.
10. S. H. Lee and M. R. Cutkosky, “Fixture planning with friction”, Transactions ASME, Journal of Engineering for Industry, 113, pp. 320–327, 1991.
11. S. Jeng, L. Chen and W. Chieng, “Analysis of minimum clamping force”, International Journal of Machine Tools and Manufacture, 35(9), pp. 1213–1224, 1995.
12. E. C. DeMeter, “The min–max load criteria as a measure of machining fixture performance”, Transactions ASME, Journal of Engineering for Industry, 116, pp. 500–507, 1994.
13. E. C. DeMeter, “Min–max load model for optimizing machining fixture performance”, Transactions ASME, Journal of Engineering for Industry, 117, pp. 186–193, 1995.
14. J. H. Fuh and A. Y. C. Nee, “Verification and optimization of workholding schemes for fixture design”, Journal of Design and Manufacturing, 4, pp. 307–318, 1994.
15. T. H. Richards, 1977, Energy Methods in Stress Analysis, Ellis Horwood, 1977.
16. M. J. Hockenberger and E. C. DeMeter, “The application of meta functions to the quasi-static analysis of workpiece displacement

within a machining fixture", Journal of Manufacturing Science and Engineering, 118, pp. 325–331, 1996.
17. M. J. Hockenberger and E. C. DeMeter, "The effect of machining fixture design parameters on workpiece displacement", Manufacturing Review, 8(1), pp. 24–32, 1995.
18. X. Gui, J. Y. H. Fuh and A. Y. C. Nee, "Modeling of frictional elastic fixture–workpiece system for improving location accuracy", IIE Transactions, 28, pp. 821–827, 1996.
19. B. Li, S. N. Melkote and B. B. Seth, "An elastic contact model for the prediction of fixture workpiece contact forces", Proceedings of the Japan-USA Symposium on Flexible Automation, Vol. 3, pp. 1243–1250, 1998.
20. J. F. Hurtado and S. N. Melkote, "A model for the prediction of reaction forces in a 3–2-1 machining fixture", Transactions of NAMRI/SME, 26, pp. 335–340, 1998.
21. B. Li and S. N. Melkote, "Improved workpiece location accuracy through fixture layout optimization", International Journal of Machine Tools and Manufacture, 39, pp. 871–883, 1999.
22. B. Li, S. N. Melkote and S. Y. Liang, "Analysis of reactions and minimum clamping force for machining fixtures with large contact areas", International Journal of Advanced Manufacturing Technology (to appear), 1999.
23. K. L. Johnson, 1985, Contact Mechanics 1st edn, Cambridge University Press.
24. P. J. Fleming and A. P. Pashkevich, "Computer aided control system design using a multi-objective optimization approach", 1985 Control Conference, Cambridge, UK, pp. 174–179, 1985.
25. P. E. Gill, W. Murray and M. H. Wright, Practical Optimization, Academic Press, 1997.
26. R. E. DeVor and S. G. Kapoor, EMSIM, http://mtamri.me.uiuc.edu/.